

Case Report

Catheter ablation of three macroreentrant atrial tachycardias after surgical repair of Double-Outlet Right Ventricle

Tadashi Wada, MD^{a,b,*}, Atsuyuki Watanabe, MD^a, Yuji Koide, MD^a, Kenzo Kagawa, MD^a, Yoichiro Naito, MD^a, Sho Tsushima, MD^a, Hironobu Toda, MD^a, Satoshi Kawada, MD^a, Ritsuko Terasaka, MD^a, Makoto Nakahama, MD^a, Satoshi Nagase, MD^b

^a Department of Cardiology, Fukuyama City Hospital, Hiroshima, Japan

^b Department of Cardiovascular Medicine, Okayama University Graduate School of Medicine, Dentistry, and Pharmaceutical Sciences, Okayama, Japan

ARTICLE INFO

Article history:

Received 20 December 2011

Received in revised form

16 January 2012

Accepted 22 January 2012

Available online 27 April 2012

Keywords:

Macroreentrant atrial tachycardia

Double-Outlet Right Ventricle

CARTO3 system

Radiofrequency ablation

Conventional mapping techniques

ABSTRACT

A 54-year-old man with a surgically repaired double-outlet right ventricle (DORV) presented with palpitations and worsening right heart failure. His 12-lead ECG showed atrial tachycardia (AT) with an atrial cycle length (CL) of 300 ms and an inverted saw-tooth F-wave pattern in the inferior leads II, III, and aVF typical of atrial flutter. Electrophysiological study and radiofrequency catheter ablation were performed. A total of 3 sustained ATs (AT1–AT3) were induced. Using the electroanatomical mapping system, CARTO3, and conventional mapping techniques, the ATs were identified as macroreentrant tachycardias circling around an incisional line on the free wall of the right atrium (AT1), the tricuspid annulus (AT2), and low voltage area in the lateral wall including the right septum (AT3). Accuracy of CARTO3 in three-dimensional reconstruction was sufficient to elucidate anatomical features (including catheter sites, incision, and low voltage areas) and macroreentrant circuits. However, conventional mapping techniques were also necessary to identify the mechanism of the tachycardias, and therefore to eliminate all of them successfully. This case demonstrates that the use of combined conventional and electroanatomical mapping techniques, such as CARTO3, can be helpful in identifying the critical isthmus for catheter ablation of macroreentrant AT in patients with surgically corrected congenital heart disease (CHD).

© 2012 Japanese Heart Rhythm Society. Published by Elsevier B.V. All rights reserved.

1. Introduction

Macroreentrant right AT occurs commonly after surgical correction of CHD [1–4]. The mechanism often suggested is a re-entry circuit around surgical scars and/or anatomic barriers [5]. Electroanatomical mapping with extensive reference to the spatial geometry of the mapped atrial chamber is useful in delineating the tachycardia isthmus of peratriotomy circuits [6,7]. For a patient with surgically corrected CHD, the anatomic position of the atriotomy scar as the arrhythmogenic substrate is commonly found in the free wall, and not in the septum [8]. The cause of this large area of low voltage (“atrial myopathy”) is still unclear, and is not always consistent with surgical trauma (incisions or cannulation sites) [8]. To identify the mechanism of the circuits of tachycardias, local electrograms must be carefully assessed in combination with conventional mapping techniques.

We describe a patient with a surgically repaired DORV in whom the use of a combined conventional and electroanatomical mapping technique, CARTO3, was helpful for identification of the critical isthmus for catheter ablation of 3 macroreentrant tachycardias.

2. Case report

A 54-year-old man with a surgically repaired DORV was admitted to our hospital due to palpitations and worsened right ventricular heart failure. He had been diagnosed with DORV and had undergone the Blalock Taussig operation at 7 years of age. He underwent the Rastelli operation at 35 years of age, with a repeat Rastelli operation at 42 years of age. A 12-lead ECG on this admission showed AT with an atrial cycle length (CL) of 300 ms, and an inverted saw-tooth F wave pattern was identified in the inferior leads II, III, and aVF, typical of atrial flutter. His chest X-ray showed cardiomegaly with a cardiothoracic ratio of 61% and mild pulmonary congestion. Transthoracic echocardiography confirmed severe right atrial (RA) and ventricular dilatation. Continuous-wave Doppler examination from the left apical 4-chamber view identified

* Corresponding author at: Department of Cardiology, Fukuyama City Hospital, 5-23-1 Zaou-chou, Fukuyama, Hiroshima 721-8511, Japan. Tel.: +81 8 4941 5151; fax: +81 8 4941 5159.

E-mail address: qq2z6qz59@tea.ocn.ne.jp (T. Wada).

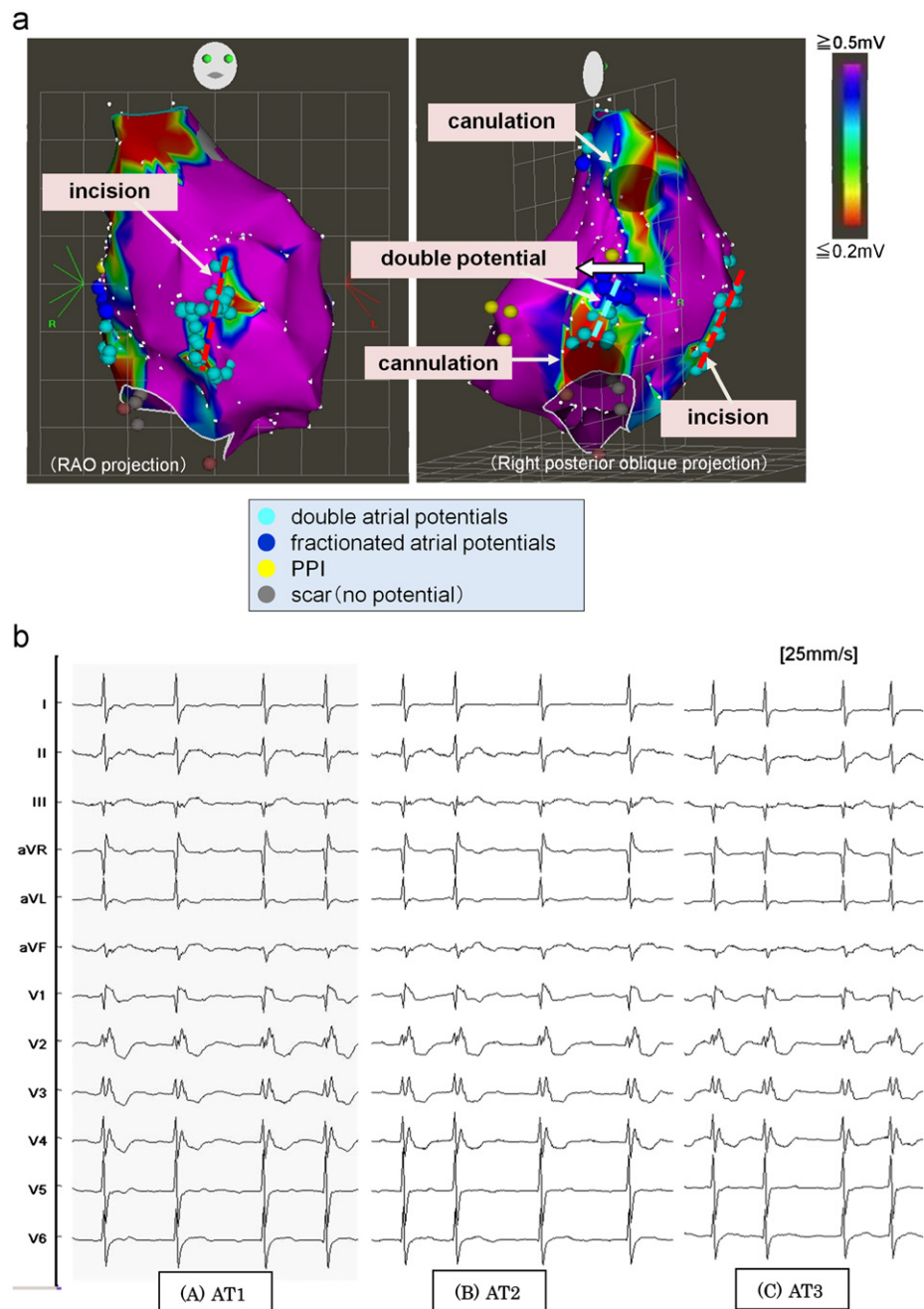


Fig. 1. (a) 3D Voltage map shows a vertical line with double potential on the RA free wall in the RAO projection, suggesting an incisional line (red dotted line). In the right posterior oblique projection, a large low-voltage area is shown on the RA postero-lateral wall, suggesting to involve the lesions with cannulations inserted (black circled area). In the middle of the low-voltage area, a vertical line (blue dotted line) with double potential and fractionated potential was shown. RAO: right anterior oblique. PPI: post pacing interval. (b) Twelve-lead ECG in AT1, AT2, and AT3.

marked tricuspid insufficiency with a systolic pressure gradient across the tricuspid valve of 40 mmHg.

After written informed consent was obtained, an electrophysiological study was performed absent antiarrhythmic agents. Electrode catheters were inserted percutaneously and positioned at the His bundle region and coronary sinus. A 20-pole electrode was placed along the tricuspid annulus (TA). An 8 F 4-mm-tip radiofrequency electroanatomical mapping/ablation catheter (Navistar, Biosense Webster, Inc.) was used for mapping and ablation. Surface and intracardiac electrocardiograms from catheters were amplified, filtered (30–500 Hz), monitored, recorded, and analyzed using Bard Electrophysiology equipment (BARD, Inc.). Electrical stimulation was performed using BC02, a digital stimulator (Fukuda, Denshi, Inc.).

Three-dimensional activation sequence mapping was performed during ATs with a CARTO3 mapping system (Biosense Webster, Inc.). The 3D geometry of the right atrium was reconstructed in real time with the electrophysiologic data, which was colored and superimposed on an anatomic map. Mapping was completed when a sufficient number of points to account for 90% of the tachycardia cycle length (TCL) had been acquired to determine the circuit during the AT [9]. The area without recordable activity or a bipolar voltage amplitude of $<0.05\text{ mV}$ was identified as scar and appeared gray on the 3D activation map. Low-voltage regions were defined by the presence of a bipolar voltage of $<0.5\text{ mV}$, as reported elsewhere [9–11]. The regions around the low-voltage area and scar were mapped

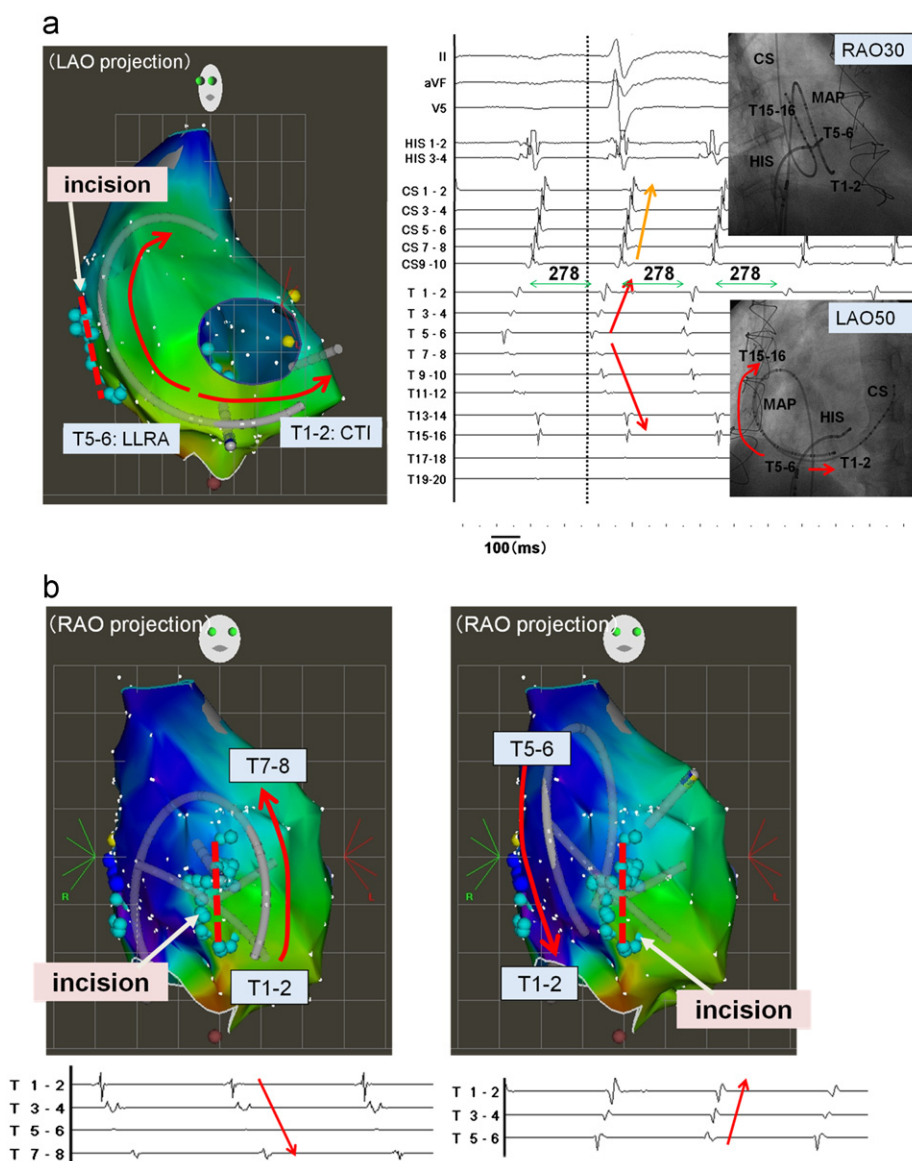


Fig. 2. (a) Right panel: Image and intracardiac electrogram during AT1 (TCL=278 ms). The earliest atrial activation was observed in LLRA. The atrial activation propagated in the distal direction to CTI and in the proximal direction along the incisional line. Left panel: CARTO3 activation map with catheters at the same time recording the right panel electrogram. LLRA: lower left right atrium. CTI: cavotricuspid isthmus. CS: coronary sinus. (b) CARTO3 activation map with catheters and intracardiac electrogram in front and behind the incisional line during AT1. Right panel: The atrial activation propagated from T1-2 to T7-8, going up in front of the incision. Left panel: The atrial activation propagated from T5-6 to T1-2, going down behind the incision.

carefully to delineate the border between 2 areas. Automatically assigned activation times were manually verified and corrected when necessary, and a single activation time was contextually assigned for fractionated and double-spiked potentials on the basis of simultaneous tip unipolar signals and surrounding activation.

The 3D voltage map, performed during AT, is shown in Fig. 1(a). It shows a vertical line with double potential on the RA free wall in the RAO projection, suggesting an incisional line. In the right posterior oblique projection, a large low-voltage area is shown on the RA posterolateral wall, appearing to involve the lesions from cannulation of the superior vena cava (SVC) and inferior vena cava (IVC). In the middle of the low-voltage area, there was a vertical line with double potential and fractionated potential. The operative records showed that the incisional line was positioned on the RA free wall and SVC and IVC cannulas of were inserted into the RA. Our estimated incisional line and the

lesions of cannulation coincided with the sites described in the operative report.

AT1 (Fig. 1b(A)) was observed on initiation of the procedure. The intracardiac electrogram during AT1 is shown in Fig. 2(a). The earliest atrial activation was observed in the lower anterior RA. The atrial activation propagated in the distal direction to the cavotricuspid isthmus (CTI) and in the proximal direction along the incisional line. It was easier to understand this propagation on the CARTO3 map. Fig. 2(b) shows the activation in front of and behind the incisional line. On the CARTO3 map, which shows the position of the catheters and the anatomical construction accurately, it is possible to interpret this activation going up in front of the incision and down behind the incision. The 3D activation map suggested that the wavefront propagated counter-clockwise around the incisional line. In addition to that, in the entrainment pacing of the tachycardia, the post pacing interval (PPI) from the 3 sites around the incisional line was identical to the TCL. AT1

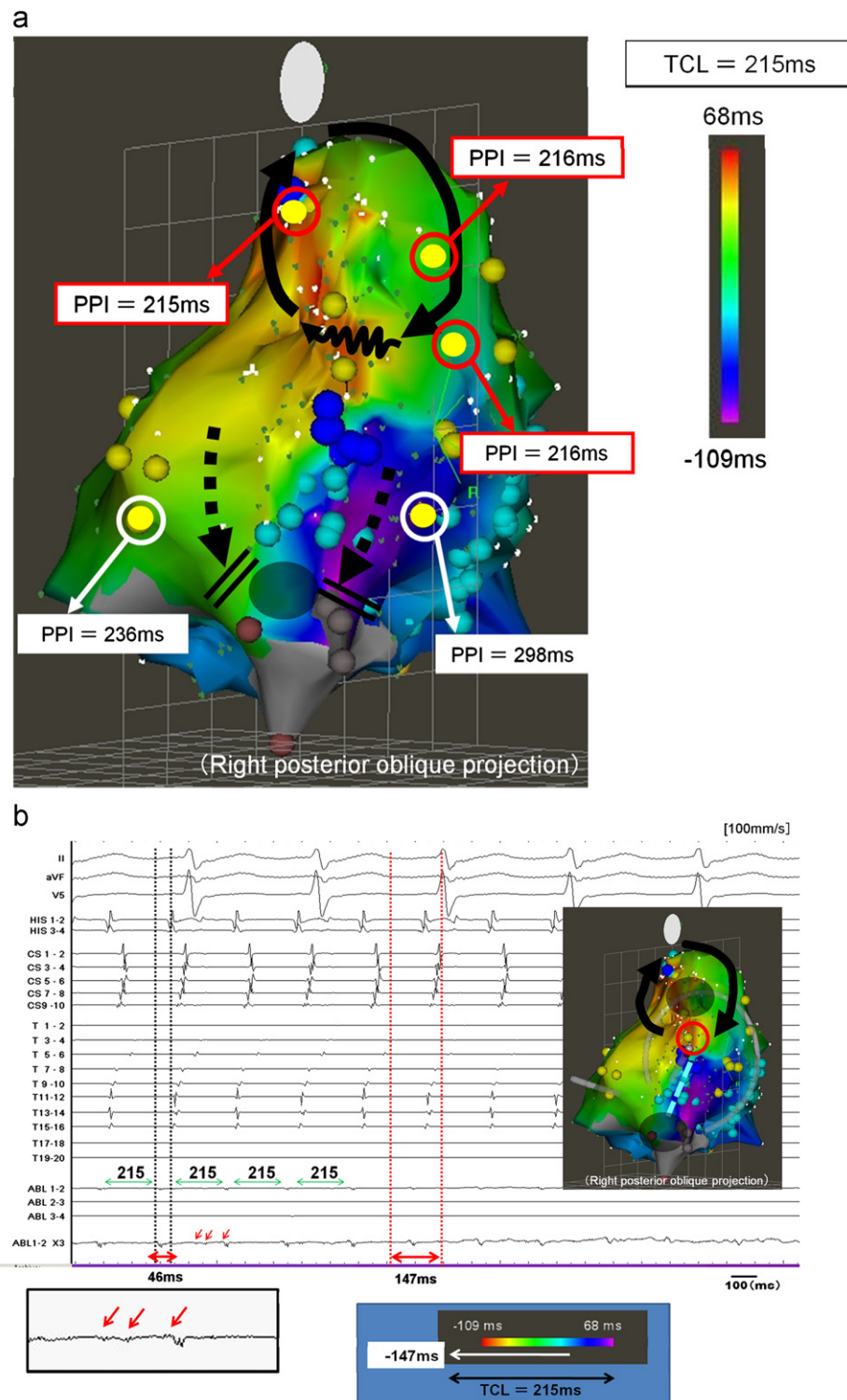


Fig. 3. (a) CARTO3 activation map of AT3 in right posterior oblique projection. PPI from the three sites around the low voltage area on the postero-lateral wall was identical to TCL. The upper wavefront (circled arrow) propagated clockwise around the low-voltage area and the two lower wavefronts (dotted arrows) terminated with blind alley. PPI: post pacing interval. TCL: tachycardia cycle length. (b) Intracardiac electrogram during AT3 with the ablation catheter positioned at the site of the estimated slow conduction (red circle on CARTO3 activation map). The slow potential with onset 46 ms before the earliest atrial potential was recorded from the ablation catheter. The two pre-potentials (arrows) were recorded ahead of the slow potential. Lower panel shows a window of activation time of AT3. In accounting the local activation time of the first pre-potential (147 ms earlier before the reference atrial potential), the window of activation time covered with TCL (215ms). TCL: tachycardia cycle length.

was identified as a macroreentrant tachycardia circling around an incisional line, and an ablation line was made between the bottom of the incision and the IVC. AT1 was terminated.

Sustained AT2 (Fig. 1b(B)) was induced during pacing from the coronary sinus. The 3D activation map and the entrainment

mapping including PPI from the CTI identified AT2 as a macroreentrant tachycardia circling counter-clockwise around the TA. AT2 was eliminated by CTI ablation.

Sustained AT3 (Fig. 1b(C)) was induced during pacing from the coronary sinus. In AT1 and AT2, a sufficient number of points

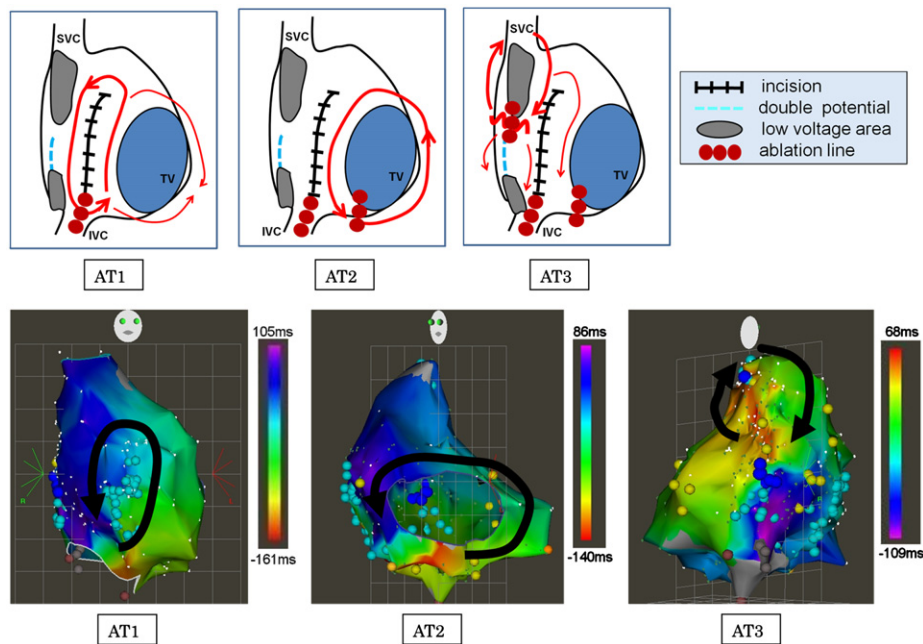


Fig. 4. Upper panel: The schema of the macroreentrant circuits in AT1, AT2, and AT3. Lower panel: CARTO3 activation map of AT1, AT2, and AT3.

(AT1, 309; AT2, 442) were acquired to determine the circuit during the AT. However, in AT3, the activation sequence could not cover the TCL, in spite of acquiring a sufficient number of points (696). As shown in Fig. 3(a), the 3D activation map roughly suggested that the wavefront propagated centrifugally from the middle of the posterolateral wall, or propagated clockwise through the right septum around the SVC and the low-voltage area on the posterolateral wall. In the entrainment pacing, the PPI from the 3 sites around the low voltage area was identical to the TCL (Fig. 3(a)), and AT3 was identified as macroreentrant tachycardia, not focal AT. As shown in the voltage map, the fractionated potential shown in the middle of the low-voltage area suggested a zone of slow conduction critical for the perpetuation of the circuit. It suggested that the upper wavefront from this slow conduction propagated clockwise around the low-voltage area and the lower one terminated on the lower posterolateral wall due to the scar from IVC cannulation. Finally, a slow potential, with onset of 46 ms before the earliest atrial potential, was recorded with the ablation catheter at the site of the estimated slow conduction (Fig. 3(b)). In addition, 2 pre-potentials were recorded ahead of the slow potential. The first pre-potential was demonstrated 147 ms earlier than the atrial potential at the distal electrode of the coronary sinus, which is defined as the reference atrial potential on the 3D activation map. In accounting for this local activation time, the window of activation time of AT3 was covered and became equal to the TCL (215 ms). Radiofrequency waves were delivered at this site, and AT3 was terminated. We ensured that this site was not too close to sinus node before ablation in sinus rhythm. An ablation line was made across the arrhythmogenic channel between the bottom of the low voltage area and the lower double potential. No tachycardia could be induced by either extra-stimulation or rapid atrial pacing (up to 300/min). At the end of the session, we confirmed that no sinus node dysfunction was present. So far, the patient has been free from palpitations for 6 months. No tachy or bradyarrhythmia has been documented, even in the Holter ECG.

3. Discussion

In this patient with a surgically repaired DORV, 3 macroreentrant ATs (AT1–AT3) were diagnosed and eliminated successfully.

Macroreentrant right AT occurs commonly after surgical correction of CHD [1–4]. The mechanism often suggested is re-entry around surgical scars and/or anatomic barriers [5]. The circuits we assumed for the 3 macroreentrant tachycardias are shown in Fig. 4. The ATs were identified circling around an incisional line on the free wall of the right atrium (AT1), the tricuspid annulus (AT2), and a low voltage area in the lateral wall including the right septum (AT3). Isthmus-dependent atrial flutter, like AT2, and intra-atrial reentrant tachycardia, like AT1 and AT3, are the most common mechanisms of atrial reentrant tachyarrhythmias in patients with surgically corrected CHD, and they frequently coexist. The surface ECG is an inefficient tool for identifying patients with coexistent arrhythmias. It has been reported that coexistent isthmus-dependent atrial flutter and intra-atrial reentrant tachycardia were found in 44% of the patients examined, while intra-atrial reentrant tachycardia alone was inducible in 37% of the patients, and isthmus-dependent atrial flutter alone in 19% [5].

Accurately understanding arrhythmogenic substrate and the anatomical construction (catheters, incision, and low voltage areas) appears to be important to assist with catheter ablation of peritriotomy circuits in CHD, as reported elsewhere [7–9]. The 3D voltage map (Fig. 1(a)) methodically performed during AT was helpful in this case. An electroanatomical map with a very high density enabled us to accurately localize the entire reentrant circuit and the arrhythmogenic channels, especially in AT1 and AT2. In addition to that, the CARTO3 map was able to accurately indicate the position of the catheters and the anatomical construction. As shown in Fig. 2(b), it was easy to detect the activation around surgical scars and/or anatomic barriers. It has been reported that electroanatomical mapping is useful to delineate a tachycardia isthmus in peritriotomy circuits [7–9]. Accuracy in three-dimensional reconstruction of CARTO3 may also be more useful to understand anatomical construction and macroreentrant circuits.

In patients with surgically corrected CHD, the anatomic position of the atriotomy scar as the arrhythmogenic substrate is commonly found in the free wall and not in the septum [8]. The cause of this large area of low voltage (“atrial myopathy”) is unclear. Possible explanations include interruption of arterial supply and insufficient

protection during cardioplegia. The multiple dense scars may result from the atriotomy, cannulation sites, conduit sites, and other surgical trauma [8]. AT3 was identified as a macroreentrant tachycardia circling through the right septum around the SVC and the large area of low voltage in the lateral wall. In the electro-anatomical map, the activation sequence could not cover the TCL in spite of acquiring a sufficient number of points. This is because the assessment of local electrograms, especially in low voltage areas, was incorrect. As noted, in cases of surgically corrected CHD, large areas of low voltage are not always consistent with surgical trauma (incisions or cannulation sites) [8]. To identify the mechanism of the circuits of AT3, it was useful to assess local electrograms carefully in combination with conventional mapping techniques. The circuit we assumed for AT3 is shown in Fig. 4. The circuit is not definitive in AT3. As our mapping and measurement of the PPI from the sites around the SVC, especially around the right septum and the junction between RA and SVC, was insufficient, we could not correctly identify whether the circuit of AT3 included the SVC or not. Considering our results from the activation map and the PPI, we assumed that AT3 was propagated clockwise around the SVC and the low-voltage area on the posterolateral wall through the right septum. The so-called “dual-loop” or “8-shaped” atrial re-entry circuit described late after correction of CHD were not found in this case [6,12,13].

Entrainment pacing was used to confirm that the tissue generating the isolated diastolic atrial potential was located within the reentrant circuit. In one series of patients with macro-right ATs following surgical repair of CHD, ablation of the isolated potentials successfully eliminated at least 1 of the ATs in 73% of the patients. However, AT recurred in 53% of these patients (mean time to recurrence 4.1 months). The use of well-referenced electroanatomical mapping to delineate the arrhythmogenic substrate clearly indicated to us the feasibility of successful ablation [14,15]. In addition, accuracy in 3D reconstruction with CARTO3 allowed us to understand the anatomical construction (catheter sites, incision, and low voltage areas) and macroreentrant circuits. Because the reentrant circuits commonly have some relationship with large areas of low voltage suggesting “atrial myopathy”, the assessment of local electrograms in low voltage areas is essential [16]. Therefore, conventional mapping techniques were also necessary to identify the mechanism of the tachycardias and to eliminate all tachycardias successfully. This case demonstrates that the use of a combined conventional and electroanatomical mapping technique, such as CARTO3, can be helpful for identification of the critical

isthmus for catheter ablation of macroreentrant AT in patients with surgically corrected CHD.

Conflict of interest

There are no conflicts of interests in this study.

References

- [1] Balaji S, Johnson TB, Sade RM, et al. Management of atrial flutter after the Fontan procedure. *J Am Coll Cardiol* 1994;23:1209–1215.
- [2] Flinn CJ, Wolff GS, Dick M, et al. Cardiac rhythm after the Mustard operation for complete transposition of the great arteries. *N Engl J Med* 1984; 21:1635–1638.
- [3] Garson Jr. A, Bink-Boelkens M, Hesslein PS, et al. Atrial flutter in the young: a collaborative study of 380 cases. *J Am Coll Cardiol* 1985;6:871–878.
- [4] Kanter RJ, Garson Jr. A. Atrial arrhythmias during chronic follow-up of surgery for complex congenital heart disease. *Pacing Clin Electrophysiol* 1997;20:502–511.
- [5] Akar JG, Kok LC, Haines DE, et al. Coexistence of type I atrial flutter and intra-atrial re-entrant tachycardia in patients with surgically corrected congenital heart disease. *J Am Coll Cardiol* 2001;38:377–384.
- [6] Seiler J, Schmid DK, Irtel TA, et al. Dual-loop circuits in postoperative atrial macro re-entrant tachycardias. *Heart* 2007;93:325–330.
- [7] Triedman JK, Alexander ME, Berul CI, et al. Electroanatomic mapping of entrained and exit zones in patients with repaired congenital heart disease and intra-atrial reentrant tachycardia. *Circulation* 2001;103:2060–2065.
- [8] Nakagawa H, Shah N, Matsudaira K, et al. Characterization of reentrant circuit in macroreentrant right atrial tachycardia after surgical repair of congenital heart disease: isolated channels between scars allow focal ablation. *Circulation* 2001;103:699–709.
- [9] Abrams DJ, Earley MJ, Sporton SC, et al. Comparison of noncontact and electroanatomic mapping to identify scar and arrhythmia late after the Fontan procedure. *Circulation* 2007;115:1738–1746.
- [10] Kistler PM, Sanders P, Fynn SP, et al. Electrophysiologic and electroanatomic changes in the human atrium associated with age. *J Am Coll Cardiol* 2004;44:109–116.
- [11] Takahashi Y, O'Neill MD, Hocini M, et al. Effects of stepwise ablation of chronic atrial fibrillation on atrial electrical and mechanical properties. *J Am Coll Cardiol* 2007;49:1306–1314.
- [12] Shah D, Jais P, Takahashi A, et al. Dual-loop intra-atrial reentry in humans. *Circulation* 2000;101:631–639.
- [13] Magnin-Poull I, De Chillou C, Miljoen H, et al. Mechanisms of right atrial tachycardia occurring late after surgical closure of atrial septal defects. *J Cardiovasc Electrophysiol* 2005;16:681–687.
- [14] Triedman JK, Saul JP, Weindling SN, et al. Radiofrequency ablation of intra-atrial reentrant tachycardia after surgical palliation of congenital heart disease. *Circulation* 1995;91:707–714.
- [15] Jais P, Shah DC, Haissaguerre M, et al. Mapping and ablation of left atrial flutters. *Circulation* 2000;101:2928–2934.
- [16] Morton JB, Sanders P, Vohra JK, et al. Effect of chronic right atrial stretch on atrial electrical remodeling in patients with an atrial septal defect. *Circulation* 2003;107:1775–1782.